Electr Eng
DOI 10.1007/s00202-008-0104-8

ORIGINAL PAPER

Conceptual design of a novel arcless controlled switch

P. Pourmohamadiyan · K. Niayesh

Received: 12 March 2008 / Accepted: 16 August 2008

Abstract A new current controlled switch is introduced in this paper and its conceptual design approach is described. The device works based on the motion of a liquid conducting medium and uses the built in electromagnetic quantities instead of external feedback signals to control the desired quantities. At first, the proposed electromagnetic structure of the device and the design criteria are introduced. After that the resulted Lorentz force on the moving conducting medium is calculated using FEM software and the motion equations of this conducting medium are solved using a numerical method. Accordingly the design criteria, which are converted to a set of mathematical and physical constraints, can be checked in each time step and the structure or quantities can be modified where needed. Finally some modifications are applied to the design and the switch operation is simulated for some different operating points.

Keywords Current controlled switch · Arcless commutation · Liquid metal motion

1 Introduction

Power systems and equipment naturally operate at multiple voltage and current levels. In addition to the many important systematical necessities, it is almost known as an unassailable rule that the voltage and the current of all equipment shall be maintained within an acceptable range. Accordingly, many control systems have been deigned to keep the system quantities in the desirable limit. Most of these control systems, through evaluation of a set of feedback signals, change some parameters in the electromagnetic devices to reach the appropriate system behavior. These signals are usually driven from the converted built-in quantities of the electromagnetic devices, like voltage and current (in accordance with magnetic flux density and magnetic flux intensity). Examples of such systems can be seen in some of FACTS devices (e.g., current and voltage controlled reactors); on load tap changers (OLTC), motor starters, etc. In some of these systems it is feasible to directly use the built-in parameters as feedback and abstain from converting the parameters. Through this simplifying idea [1], the designer may combine or even eliminate some parts of the above mentioned system. This technique may decrease the production costs and also facilitate the operation, especially when the equipment is distributed extensively in the system. Considering to the widespread nature of the power systems and industrial plants, in such cases, it is almost impossible to use the conventional measuring devices and control circuits which indeed require more precise maintenance and take much space. Up to now, due to the aforesaid difficulties, it was ignored to apply the complicated control systems on the down-stream side or less important equipment of the system (e.g., using OLTC on the distribution transformers). Most of these missed control systems can be realized via soft switching of current from one part of the circuit to another part in proper time and appropriate way.

In this paper, the conceptual design of an arcless current/voltage controlled switch is introduced. The switch operates via movement of liquid metal. Liquid metal movement has already been used in some applications and researches.

P. Pourmohamadiyan · K. Niayesh
School of Electrical and Computer Engineering,
University of Tehran, Campus #2, P.O. Box 14395-515,
14395 Tehran, Iran
e-mail: kniayesh@ut.ac.ir

P. Pourmohamadiyan (✉)
2nd Floor, No. 55 of Fifth Dd. Court, Navid Alley,
Ostad_Nejatollahi Street, Tehran, Iran
e-mail: pmohmad@ut.ac.ir

The most recent and similar one uses the fast movement of the liquid metal for gradual change of resistance and current limitation [2]. In the mentioned application, the most important concern is to limit the fault current as fast as possible without any arc. In the present research the movement of the liquid metal is not so fast because it should be controlled and settled at specific contacts when the required condition is fulfilled. For this purpose a special structure is proposed and a FEM solver is used for calculation of the electromagnetic quantities and Lorentz force. The normal and abnormal voltage and currents of the circuit are assumed as excitations of the system. Then movement equations of the liquid metal are solved using a numerical method and the design criteria are checked in various steps. The structure or design parameters are changed where needed. Finally to demonstrate the described principal, performance of the designed switch is simulated for a hypothetical operating point. The worked example shows that the switch can be made with dimensions of a few centimeters and can operate in the range of 40–50 A of current without occurrence of undesirable phenomenon. The proposed technique can be used as a basic idea to design a new and simple OLTC for low voltage transformers. The design method introduced in this paper has several advantages compared to the conventional designs of switches, such as no need to external triggering system, much more compact sizes, no degradation of the contact system, e.g., due to the arcing and no drive mechanism.

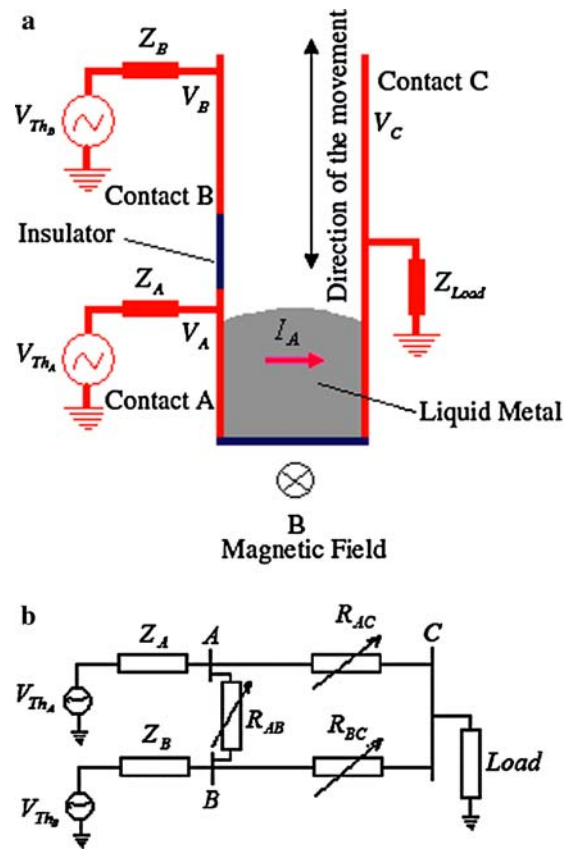

Fig. 1 **a** Basic schematics of the working principle of the device. **b** Equivalent circuit of the device

2 Problem description

Regardless of the type and application of the equipment, this paper is intended to present a design method for arcless commutation of current between contacts with known equivalent Thevenin impedances and voltages. The switch operates during transition from normal condition to abnormal condition (in our case unacceptable voltages and currents are assumed as abnormal conditions). The current commutates between two contacts, via the movement of a movable conducting medium under the effect of Lorentz force resulted from the interaction of the flowing current and a magnetic field which is also proportional to the flowing current. Figure 1 illustrates the basic scheme of the device operation and its equivalent circuit.

The parameters of the equivalent circuit shown in Fig. 1 are defined as:

- The nominal RMS value of Sinusoidal Steady State currents which flow through contact A or B during equilibrium (normal) condition are denoted by I_A and I_B respectively.
- The nominal RMS value of Sinusoidal Steady State voltages of contacts A and B during equilibrium (normal) condition are denoted by V_A and V_B respectively.
- All of the mentioned quantities during abnormal conditions (unacceptable currents and voltages), which shall lead to change over between contacts, are denoted by the same primed designation (e.g., I'_A, I'_B etc.).
- Z_A and Z_B represent the equivalent Thevenin impedances of the sources behind contacts A and B respectively.
- R_{AC} and R_{BC} represent the equivalent variable resistances between the common contact C and contacts A and B respectively. During the current commutation one of these resistances gradually increases while the other one decreases.
- R_{AB} is the variable resistance between contacts A and B. When the system is in normal operation, this resistance is very large (almost infinity). During the current commutation and while R_{AC} and R_{BC} are undergoing the prescribed variations, this resistance gradually decreases and reaches to its minimum value and after that (when the current completely is commutated) it increases and so contacts A and B are disconnected again.

The device has to be designed based on the following criteria:

1. The movable conducting medium must be remained stationary when the system quantities are in equilibrium (normal) conditions. In other words, when the system operates at acceptable voltage and current, the current shall not commutate.
2. The movable conducting medium should be ready to move when the system quantities are out of the normal condition. From the physical point of view, it means that the resulted net force on the movable conducting medium tends to be increased in a direction which will bring the system to another equilibrium condition.
3. The movable conducting medium must start to move once the system quantities reach to predetermined abnormal values (threshold values of voltage and current).
4. During the commutating phase, thermal stressing must be avoided in the tail of movable conducting medium. In other words, the voltage drop on this part of circuit must be limited to a specified $V_{\max}$(like the boiling voltage for conventional separating contacts [3]).
5. During the commutating phase, the difference between the applied voltages on the separating contacts should not exceed a minimum level $V_{\min}^{\text{arc}}$ (dependent on the contacts material [4]).
6. When the current completely commutates and the system reaches to a new equilibrium condition, the net exerted force and the speed of the movable conducting medium must be zero.
7. The voltage appears across insulation parts should not exceed their respective breakdown voltages.

3 Design and analysis of the device structure

The criteria 1, 2, 3 and 6 of the preceding chapter imply that, at each moment, there should be a set of motive and repellent forces which can interact and provide the desired conditions. As it was stated, the Lorentz force is the only motive force in the device. This force is proportional to the vector product of current density and a magnetic field density which itself is also proportional to the flowing current. Accordingly, for the first step of evaluation and design, the motive force can be estimated as:

$$F_{\text{motive}} = K_{\text{Device}} I^2 \tag{1}$$

where K_{Device} is a constant which depends on the geometry of the system (i.e., the position of the liquid metal droplet) and the contact angle. The later is defined based on the magnitude and direction of surface tension vectors. In the present design, to facilitate the control of the motion, the magnetic circuit of the device is designed in such a way that K_{Device} almost does not change during the motion, though its small variations are also taken into account. Considering to the specified normal (equilibrium) currents and using the estimated K_{Device}, the amount of needed repellent forces at equilibrium conditions can be determined. The gravitation force is used as repellent force. According to clauses 1 and 6 of the design criteria, the movable conducting medium shall be remained stationary at different normal operating points (normal voltages and currents). Since the amplitude of the normal currents differs at two contact positions, the effective component of the gravitation force (which is along the direction of motion), should be changed at these two contacts. In other word the direction of motion shall make different angles with horizontal line. An acceptable estimation for calculation of the desired slopes is that, at equilibrium states, the ratio of motive forces shall be equal to the ratio of repellent forces at different slopes of motion. Figure 2 illustrates the general structure of the device. Considering to the structure of the device, a liquid metal (LM) is selected as moving conducting medium. As it can be seen, contacts A and B are separated via a solid insulation material. In order to prevent any arc during contact separation, at first the liquid metal moves to a high resistance area which gradually decrease the current flowing through the first contact. Then, before complete separation from the first contact, the liquid metal reaches to another high resistance area which is connected to the second contact. As a result of the movement, the current flowing through the second contact will gradually increase. The amount of these high resistances and their length should be evaluated through numerous compromises between different technical constraints.

3.1 Liquid metal dynamics

Movement of liquid metal has been used in some engineering applications and its characteristics are well recognized [5–7] but due to the type of applications, existing researches mostly deal with the steady flow characteristics of the liquid metals. In the present study, the applicable results of [8] are considered in the design of device structure. The physical and fluid flow data are extracted from [9] and due to the similarity of application the governing equation of motion dynamics is extracted from [10].

Under simplifying assumption, the motion of liquid metal droplet can be approximated as a solid particle with the same mass. This simplifying assumption has been used in [2] which deals with approximately same volume of liquid metal but with higher speed and flowing current. Nevertheless, the experimental results of the mentioned research were in good correlation with the theoretical assumptions. In the present study the mesh elements are built with dimensions of 0.1 mm and number of calculation passes is set equal to ten. The present research is intended to use the movement of the liquid metal in a more stable condition with the speeds in the order of 0.1 (m/s) which is well enough to cause very thin

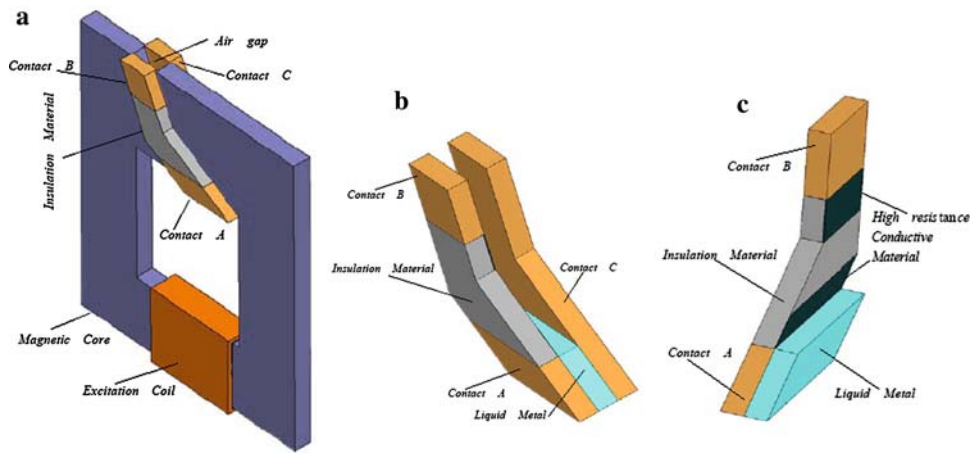

Fig. 2 Structure of the device. **a** General perspective, **b** cross section of the device, **c** detail view of the contact system

boundary layer during motion of liquid metal. So the motion dynamics of the liquid metal particle can be formulated as:

$$m_{\mathrm{LM}}\frac{\mathrm{d}^2 s}{\mathrm{d}t^2}+\alpha\frac{\mathrm{d}s}{\mathrm{d}t}=F_{\mathrm{motive}}-F_{\mathrm{repellent}}-F_p \tag{2}$$

Here, S is the position of the LM droplet, F_p represents the force produced due to pressure difference of air columns over and under the LM droplet and α is the loss factor, which is considered to take the velocity dependent breaking force into account. The liquid metal flow in the vicinity of the capillary walls is considered to be similar to the flow around a body of the length l that is drawn through a liquid. Thus a laminar layer, the so called Prandtl layer of the thickness D occurs near the capillary walls:

$$D=\sqrt{\frac{6\eta l}{\rho_{\mathrm{LM}}v}} \tag{3}$$

where ρ_{LM} is the density of LM, $\eta$is the dynamic viscosity and v is the velocity of the LM droplet. The length l of the body corresponds to the height of the LM droplet in the capillary. In our device the velocity of LM droplet is in the range of centimeter per second, $\rho_{\mathrm{LM}}=13{,}534\ \frac{\mathrm{kg}}{m^3}$,$\eta=0.001556\frac{\mathrm{kg}}{\mathrm{ms}}$ is the dynamic viscosity of Mercury and $l=7$ mm is the equivalent diameter of the LM droplet. Accordingly the resulting Prandtl layer is in the sub-millimeter range, which is much smaller than LM droplet dimensions. Hence the droplet is affected by a friction force F_{frict}

$$F_{\mathrm{frict}}=\frac{\eta A v}{D}=\alpha\frac{\mathrm{d}s}{\mathrm{d}t} \tag{4}$$

where A represents the contact surface between the LM droplet and the capillary walls. As it can be seen, this factor is depended on the velocity of the LM droplet. Therefore, in order to find the exact position and velocity of the LM droplet, the Eqs. (2) and (4) have to be solved simultaneously. For the configuration considered here, this loss factor is of about 0.0003. To verify the designed structure, the motion profile has to be checked for the condition stipulated in the design criteria. For this purpose, the start point is considered the moment at which the currents flowing through contact A reaches toI'_{A}. We assume that this sinusoidal current has an arbitrary phase angle ϕ. Then using the FEM solver, the magnetic flux and current density vectors and the resulted forces components in the three Cartesian directions (F_x, F_y *and* F_z) are calculated. Using these force components, the effective components of the motive and repellent forces can easily be calculated considering to the slope of motion. The motion starts when the right hand side of Eq. (2) becomes positive. To fulfill clause 6 of the design criteria, the net exerted force and speed shall be vanished, when the LM droplet reaches to the second equilibrium state (e.g., contact B). At this stage some design parameters (e.g., magnetic circuit, contact area, etc.) have been modified in order to meet the clauses 3 and 6 of the design criteria simultaneously. Since the motive and repellent forces values depend on the position and contact angle of the LM droplet, the right hand side of Eq. (2) is not constant. Thus the motion is broken to small time steps in which the second order differential equation of (2) can be solved with constant coefficients. At the end of each time step the calculated speed ($\frac{ds}{dt}\Big|_{t=nt_s}$) and acceleration ($\frac{d^2s}{dt^2}\Big|_{t=nt_s}$) is assumed as the initial conditions of the differential equation (2) is assumed as the initial conditions of the differential equation (2) which has to be solved for the next time step and position. Meanwhile, as explained earlier, the calculated speed has to be approximately checked with presupposed α to avoid inaccurate results. The time step is selected considering to the fact that the Lorentz force oscillates at a frequency which is twice the frequency of the flowing current. The sampling frequency (i.e., is the number of time steps per second) is much greater than twice the highest frequency of motive force variations. To assure about the successful operation of the switch, the contact angle and wettability of the LM on the solid surfaces should be evaluated. In [11], a comprehensive study has been

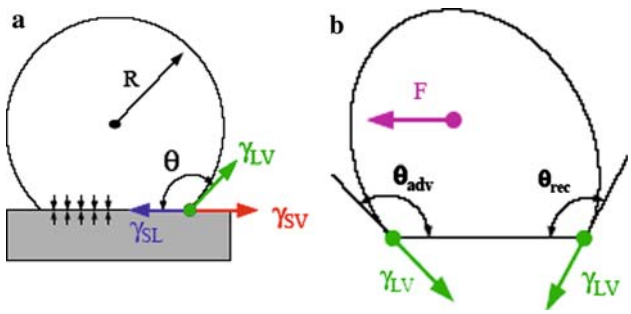

Fig. 3 **a** Contact angle of a droplet, **b** droplet under the influence of external force F

conducted on the same materials used in relatively similar dimensions. The technique has been demonstrated using the mercury–graphite system at room temperature and the contact angle was determined to be $152.5 \pm 2°$ which shows the low wettability of the LM on the used substrate. In fact since the LM droplet has to be in contact with four adjacent walls with different materials, the analytic modeling of the contact angles is very complicated. It should be considered that the contact angle oscillation is occurred due to the periodic change of the interface profile between the droplet and substrate and by the failure of Young's equation due to the change of orientations of surface and interface tensions [12]. Moreover the free surfaces of the LM droplet face with some instabilities due to the electromagnetic fields at relatively high frequencies [13]. Fortunately, in the proposed system the frequency is low and this effect can be neglected. The minimum force needed to slide the LM droplet on a solid surface can be estimated by taking the surface tensions and contact angle as shown in Fig. 3 [14].

For this purpose, the droplet is characterized by two parameters: the droplet radius and the initial contact angle described by Young's equation:

$$\gamma_{\mathrm{LV}} \cos\theta + \gamma_{\mathrm{SL}} = \gamma_{\mathrm{SV}} \tag{5}$$

where γ_{LV}, γ_{SV} and γ_{SL} are surface tensions at liquid/vapor, solid/vapor and liquid/solid interface, respectively. The force balance in Fig. 3b, expressed as Eq. (6), shows that the resistance against moving is ruled by two material parameters J and θ and one design parameter R.

$$F = \gamma_{\mathrm{LV}} \times J \times 2R \times \mathrm{Cos}\,(\pi/2 - \theta) \tag{6}$$

The J parameter may be considered as a "sliding criteria", determined by the contact-angle hysteresis, advancing (θ_{adv}) and receding (θ_{rec}) angles. Note that Eq. (6) also indicates that the force required to move a droplet, increases linearly with the droplet size. If the external force applied to the droplet is larger than the maximum resistance by the contact-angle hysteresis, the droplet moves. Based on experiments, it can be assumed that $\theta = 152.5^{\circ}$, J = 0.06 and $\gamma_{\mathrm{LV}} = 0.484$ N/m at room temperature. Accordingly the horizontal force required

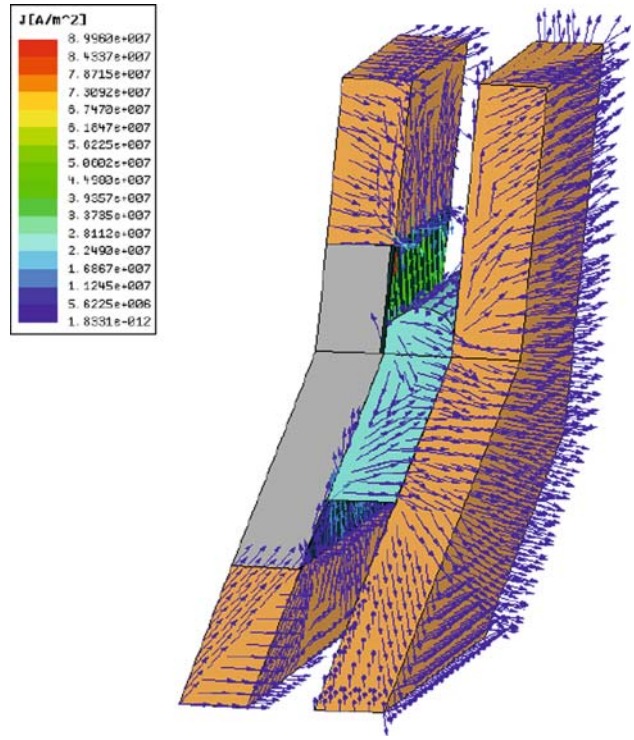

Fig. 4 Geometry and current density distribution for the worst condition during current commutation

to actuate a droplet of 3.3 mm radius is estimated at about $F = 90\ \mu$N. In the subsequent chapters, it will be demonstrated (Fig. 5c, e) that the net force exerted on the LM droplet is well greater than four times of the calculated force. This shows that the LM droplet can slide on its four-side walls and the assumption of motion modeling is not far from reality.

3.2 Thermal overstressing

To check the fulfillment of the design criteria number 4, the equivalent circuit of the device (Fig. 1b) is considered. The most difficult condition for thermal overstressing is when the thin tail of the liquid metal is separating from the end of the first contact. Considering to the Prandtl layer thickness and the speed of the motion, the worst geometry which may be occurred is simulated by the FEM solver (see Fig. 4). The resistance matrix which describes the equivalent circuit of Fig. 1 is depended on the position of LM droplet, the geometry and the contact angle. The elements of this matrix are determined by applying some special cases of voltage and currents in the FEM software and neglecting the self resistances of contacts($R_{\mathrm{AA}} = R_{\mathrm{BB}} = R_{\mathrm{CC}} = 0$).

As illustrated in Fig. 4, the worst case occurs when the LM droplet is separating from the high resistance region of contact A (made from resistive material) and is connected to the inferior part of contact B. Using the calculated resistances and

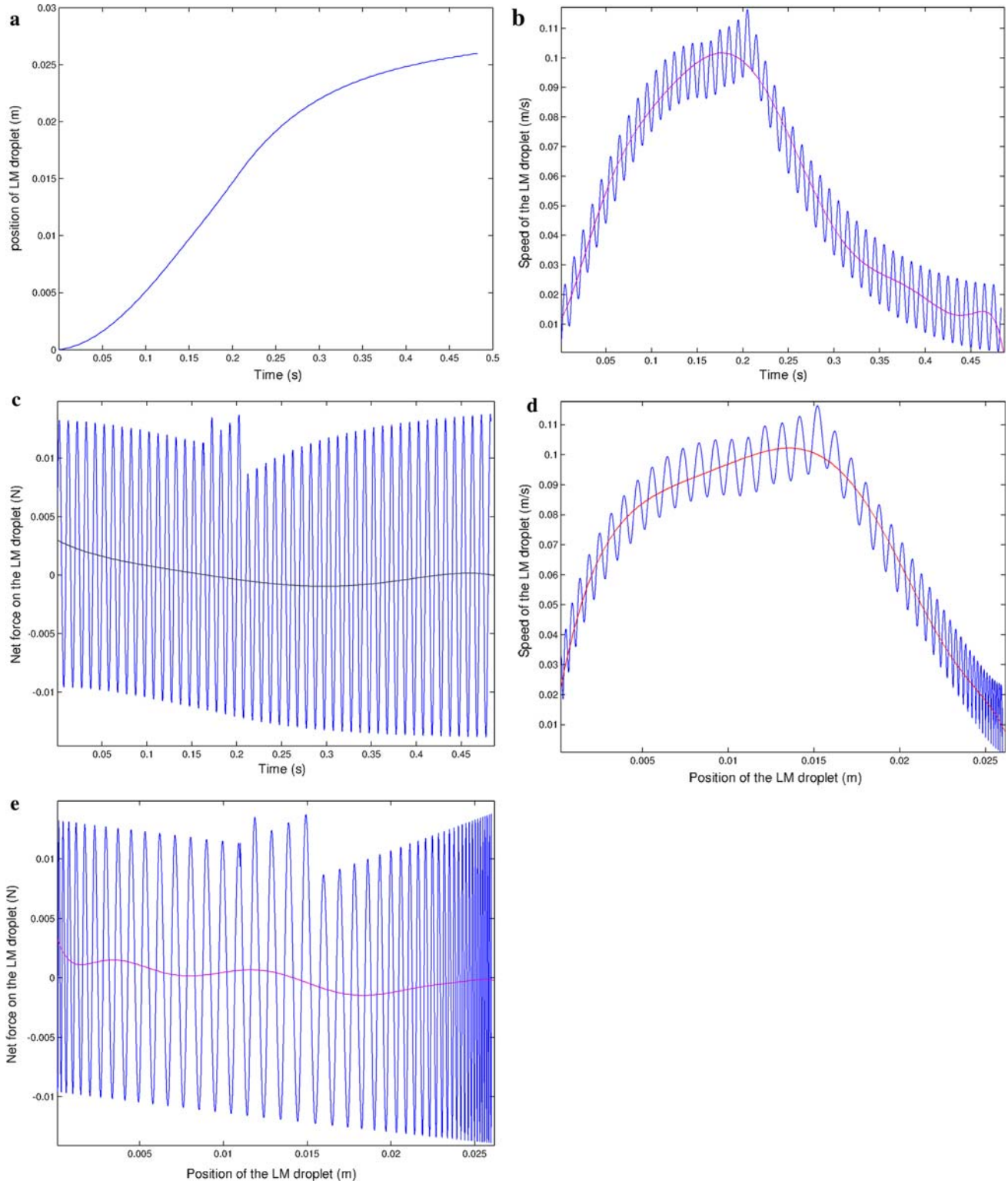

Fig. 5 **a** Position of LM droplet versus time. **b** Speed of LM droplet versus time. **c** Net force on the LM droplet versus time. **d** Speed of LM droplet versus position. **e** Net force on the LM droplet versus position

considering to the presupposed values of equivalent Thevenin voltages behind contacts, the equivalent circuit of Fig. 1b is solved. In our study, to have more operational model and realistic results, it is assumed that the active power flowing through contact C is constant during current commutation and the circuit is solved using non-linear iterative methods

used in conventional power system load flow study. The calculated voltages and currents are used as excitations of the FEM software and the heat loss in the LM tail is calculated. Within the range of operating currents, assuming adiabatic system and considering to the maximum transition time (minimum possible speed) of the LM tail, it is observed that no considerable temperature rise can be occurred in the LM. This matter is well described in the worked example. It is demonstrated that even with too much greater resistances and losses than the ones calculated, the temperature rise of the LM droplet would not reach to the critical point.

3.3 Arcless current commutation

To fulfill clause number 5 of the design criteria, again worst condition illustrated in Fig. 4 must be studied from current commutation point of view. The aim of the high resistance region of contact A is to gradually reduce the currents of contact A while the current of contact B is increasing. But to reach the correct liquid metal motion, the reduction of the current of contact A can not be unlimited. Because the speed and transition times have to be within acceptable limits which is compatible with the device application. Too much current reduction may cause low motive forces and subsequent failure of motion. Therefore there is always a minimum current at the time of contact commutation which will produce a voltage $V_{\text{Separation}}$ between the LM droplet and the contact left behind. The governing equation in this condition is:

$$V_{Th_{\text{A}}} = L_A \frac{\mathrm{d}i_{\text{A}}}{\mathrm{d}t} + V_{\text{Separation}} + V_{\text{C}} \tag{7}$$

Here V_{C} denotes the voltage of contact C (which is approximately equal to V_{B}), L_{A} denotes the equivalent total inductance behind contact A. Determination of the exact value of $\frac{\mathrm{d}i_{\text{A}}}{\mathrm{d}t}$ is relatively difficult. But it can be approximated considering the system frequency and minimum transition time (maximum possible speed). During the current commutation and while the LM is separating from the first contact, no considerable Transient Recovery Voltage (TRV) is applied across the gap since the LM droplet has already been connected to the second contact. Using Eq. (7) the maximum possible value of $V_{\text{Separation}}$ is calculated. This voltage should not exceed a minimum level $V_{\text{min}}^{\text{arc}}$ [4]:

$$V_{\text{Separation}} \langle\ V_{\text{min}}^{\text{arc}} \tag{8}$$

3.4 Forces during current commutation

To optimize the flow of the droplet [8] and to prevent undesirable discontinuity of the LM, the ratio of the height of the LM droplet to its width (the distance between the contacts) is gradually increased [2]. But during current commutation, due to the changes of the current density magnitude and direction in the tail of LM droplet, the ratios of Lorentz force components (F_x, F_y and F_z) differ from those in normal motion of the LM droplet. At this critical moment, the differences between the applied local forces must be limited in order to avoid the deformation of the LM droplet and the possible subsequent fragmentation of the droplet. To have an acceptable insight, the geometry of the LM is divided to small cubical elements. Then, the exact value and the direction of Lorentz force components are calculated for each small element. The resulted forces matrix is analyzed and accordingly the weak neighbor elements are identified. A discontinuity may be occurred if the existing forces differences prevail over the surface tension of the LM. This time consuming calculations can be limited to critical area of concern. Another important technical point is the magnitude of the force component which is perpendicular to the surface of the fixed contacts (in the present coordinate system that is F_y). This force does not affect the motion directly but can affect the current commutation between the LM droplet and fixed contacts. This force component is checked during the motion and was reduced via the change of the device structure. To have a relatively uniform Lorentz force all over the LM droplet volume, the magnetic field and current density distribution must be kept uniform.

4 Simulation results and discussion

To demonstrate the described principal, the operation of the designed structure was simulated with the following assumptions:

$$V_A = 220\ \text{V},\ I_A = 36.4\ \text{A}$$
$$V_A' = 215\ \text{V},\ I_A' = 46\ \text{A}$$
$$V_B = 228\ \text{V},\ I_B = 43.8\ \text{A}$$
$$Z_A = 1.21\ \Omega,\ Z_B = 1.33\ \Omega$$

The simulation results of the liquid metal behavior during current commutation from contact A to the contact B are shown in Fig. 5.

Figure 5a shows the position of liquid metal droplet versus time. As it can be seen the liquid metal droplet reaches the final position (which is spaced 26.2 mm apart from the start point) within 0.485 s. Figure 5b shows the instantaneous and average value of the liquid metal speed versus time. Considering to the frequency of change of instantaneous net force exerted on the liquid metal droplet (100 Hz), 0.0025 s time step intervals are selected for motion simulation. This figure illustrates that the speed of liquid metal droplet reaches zero at t = 0.485 s (when the liquid metal droplet reaches to the predetermined final position). Figure 5c shows the instantaneous and average value of the net force exerted on the liquid metal versus time. It is illustrated that the net

average force exerted on the liquid metal droplet reaches zero at $t = 0.485$ s. Figures 5d and e restate the same concepts by illustration of speed and the net force exerted on the LM versus its position. It can be seen that both of the mentioned quantities reach zero when the droplet reaches its final position (which is spaced 26.2 mm from the start point).

As it can be seen, the design criteria have been fulfilled in the device. To meet these requirements, some of the device parameters have been changed during various steps of the design. Some of the most important challenges were as follows:

1. In the preliminary designed structure, the speed of the LM droplet didn't vanish when it reached the final position (contact B), though the net force exerted on it was zero. To solve this problem, the applied motive force (Lorentz force) has been decreased in the high resistance region while this force is higher than a threshold level to hold the LM droplet at the position of contact B (to have equilibrium condition). Accordingly, the thickness of the high resistance area was decreased. As a result the resistance of this region increased to reduce the current density and Lorentz force just before entering the final position (contact B). This force reduction, in effect, reduces the average velocity of the liquid metal droplet before entering the region of contact B. Figure 6 shows the calculated speed profiles before and after the modification. This change has also facilitated the current commutation.
2. Performance of the designed structure shall be independent of the moment that the current commutation is started (phase angle of the sinusoidal current). The subject was studied by changing the current phase angle ϕ between 0° and 90° which may cause maximum possible difference in the current amplitude at the moment of current commutation. No considerable change was observed in the total transition time, final equilibrium position (i.e., $v = F_{\text{net}} = 0$) and thermal effects. But as it was expressed in Eq. (7), the magnitude of the $V_{\text{Separation}}$ is certainly dependent on this phase angle. The maximum possible value of this voltage was calculated and it was checked as stated in inequality (8). Usually the minimum arcing voltages ($V_{\text{min}}^{\text{arc}}$) of high resistance materials are high enough and the real concern is the arcing voltage of the LM. For the assumed operating points the commutation voltage is in the range of 1.5–2.5 V which is smaller than the minimum arcing voltage of the LM.
3. The LM volume was divided to small cubical elements with dimensions of 0.001 cubic millimeters. The analysis of the forces matrix of the spatial elements shows that these forces do not exceed 0.68 μN for two adjacent elements. This force is much less than the needed force to separate two LM particle with the aforesaid volume. Therefore no discontinuity would occur between the tail and the rest of the body. In the preliminary designed structure, at the commutation geometry, the force component which is perpendicular to the surface of the fixed contacts (i.e., F_y) was rather large. To reduce this force component, the width of the magnetic core was extended (from 6 to 8 mm) to produce more uniform magnetic field in the motion path. It is notable that extra extension of the magnetic core may change the current density distribution in the fixed contacts which subsequently will change the current density distribution at the interface of the LM droplet and copper contacts. From the equivalent circuit point of view, this means change of contact resistance between LM and fixed contacts. Although this resistance is much lower than the bulk resistance of the LM and external circuit [2] but if the mentioned effect can not be reduced enough this assumption will not be valid anymore.
4. To study the possible thermal stress, at first the heat loss of the system was calculated by the FEM solver. To study the worst condition and to have a safe side design, the commutation geometry of the system was selected. It was assumed that an equivalent amount of heat loss power of all parts of the device was generated by the liquid metal (i.e., less than 0.4 W). Then assuming adiabatic system the total time needed for the liquid metal to reach to the boiling temperature was calculated (i.e., 198 s) and it was observed that this time is much larger than the time needed for commutation (i.e., about 0.4 s). In the normal condition, the case is much better since the heat loss power is much less. However to approximate the liquid metal temperature rise, the thermal conduction of the elements was ignored and the steady state temperature rise of the liquid metal was calculated considering to

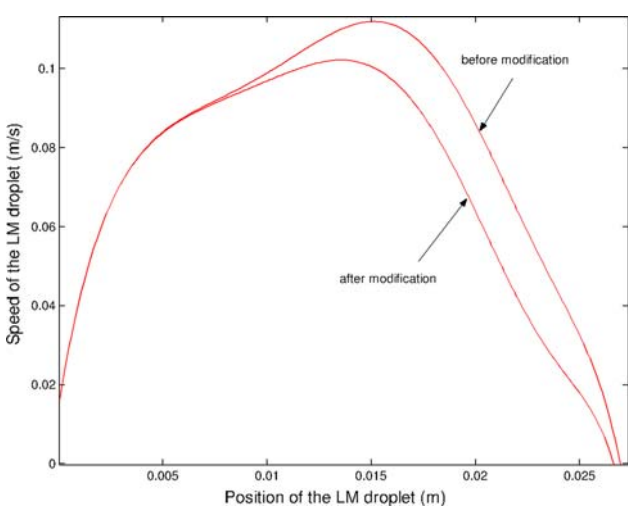

Fig. 6 Speed profiles before and after the modification (with and without change of high resistance region)

the heat convection of the liquid metal. According to Newton's law of cooling the temperature rise of the LM droplet can be calculated with the following equation [15]:

$$q = \bar{h}(T_{\text{body}} - T_{\infty}) \tag{9}$$

where q is the total heat power generated in the LM divided by the free surface area of the LM droplet, $\bar{h}$is the average heat transfer coefficient of the body (i.e., liquid metal droplet). T_{body} and T_{∞} are the temperatures of the hot body and the coolant fluid, respectively (in our case the LM is surrounded by air). The heat transfer coefficient of the LM $\bar{h}$, is in the range of $3–5\times10^5$ W/K m^2 [9]. It was observed that even with the most stringent assumptions for calculation; the temperature rise of the liquid metal would not exceed 1 K. It must be noted that the contribution of the thermal conduction would result in even less temperature rises.

5. The stability of the LM in the second equilibrium condition (contact B) was studied through a sensitivity analysis of the LM movement with respect to some transient currents with different amplitudes and durations. In the designed structure, the equilibrium condition of the LM is specified in a manner that it has a 12 mm dead band area which let the LM to be kept in contact B during 6 mm movement upward or downward. In other words, the current will flow through contact B if the liquid metal position (S) lies in the following interval (S = 26.2 mm is the normal equilibrium condition):

$$20.2\,\text{mm} \langle S \langle 32.2\,\text{mm} \tag{10}$$

Using the method described for Liquid Metal Dynamics Simulation, the maximum movements of the LM droplet due to various transient conditions were calculated. Figure 7 shows the dynamic position of the LM droplet, during an abrupt 20% reduction in current amplitude for four cycles. As it can be seen the LM droplet bounces back to its initial position.

The maximum deviation of the LM droplet during different current transients is shown in Fig. 8. In this figure the number of cycles which transient occurs, N, is used as a parameter and upper and lower limits of the movement corresponding to two directions are shown to illustrate the sustainable transients. It was observed that if the maximum duration of the transient is limited to one cycle (i.e., 0.02 s), the LM droplet will keep its contact with contact B if the transient current amplitude lies within the range of 0.08 to 2.2 times of the normal current. In an extremely critical condition, if the duration of the transient is equal to 200 ms, the LM droplet will keep its contact with contact B if the transient current amplitude lies within the range of 0.87 to 1.14 times of the normal current.

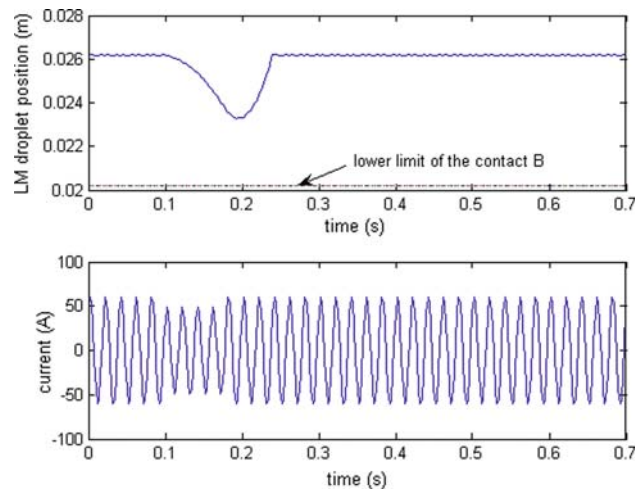

Fig. 7 Position of the LM droplet and the current flowing through the switch during an abrupt 20% reduction in current amplitude for four cycles

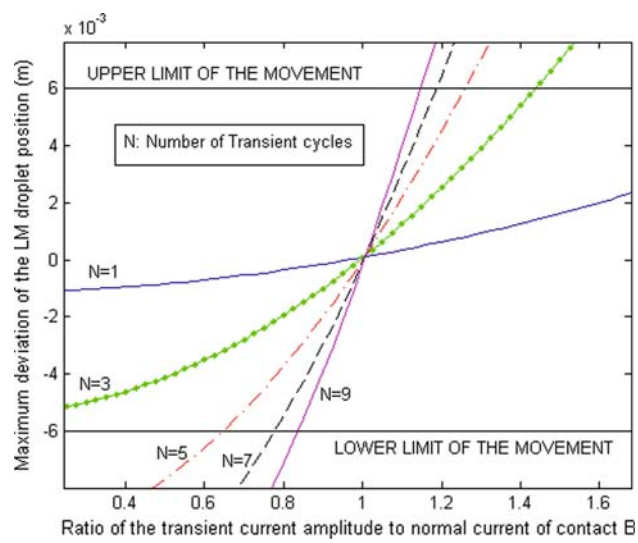

Fig. 8 Movement of the LM droplet versus the ratio of the transient current amplitude to normal current of contact B

5 Conclusions

This paper presents a novel method for arcless current commutation using liquid metals. The working principle of the proposed device is based on the motion of a liquid conducting medium under influence of built-in electromagnetic forces. The phenomena relating to the current commutation have been investigated and the relevant theoretical constraints have been derived. To validate the design, the governing equations are solved to analyze the motion of the liquid metal

and to study the failure possibility due to the undesired effects like thermal overstressing and arcing during contact separation. To consider the possible deformation of the liquid metal during its motion and its resulted influence on the current density distribution, in each time step, a finite elements simulation has been carried out. The simulation results indicate that using appropriate geometries, it is possible to design the structure of the device in such a way that all necessary operating criteria are fulfilled. Although the proposed design method needs in depth precision to fulfill all criteria but the switch takes advantage of the controllable arcless operation without external triggering, with relatively small size. Moreover due to use of liquid metal movement in the switch, some other problems of conventional switches like surface degradation of contacts and mal-operation of mechanical mechanisms can be avoided.

Acknowledgments This work was supported by Iran National Science Foundation through Grant No. 86064/26.

References

1. Niayesh K, Pourmohamadiyan P (2006) A novel technique for control of electromagnetic devices: liquid metal contact changer. In: 51st Internationales Wissenschaftliches Kolloquium, Technische Universität Ilmenau, paper 6.3–12, 11–15 September
2. Niayesh K, Tepper J, Koenig K (2006) A novel current limitation principle based on application of liquid metals. IEEE Trans Compon Packag Technol 29(2):303–309
3. Slade P (1999) Electrical contacts: principals and applications. Marcel Decker Inc., New York
4. Holm R (2000) Electric contacts: theory and applications, 4th edn. Springer, Berlin
5. Takahashi M, Momozaki Y (2000) Pressure drop and heat transfer of a mercury single-phase flow and an air–mercury two-phase flow in a helical tube under a strong magnetic field. Fusion Eng Des 51–52: 869–877
6. Davidson PA (2001) An introduction to magnetohydrodynamics. Cambridge University Press, London
7. Smolentsev S, Abdou M (2005) Open-surface MHD flow over a curved wall in the 3-D thin-shear-layer approximation. Appl Math Model 29:215–234
8. Ni M-J, Abdou M (2006) Projection and simple methods for unsteady incompressible navier–stokes equations. IHTC-13, Sydney
9. Cord H (1998) A literature survey on fluid flow data for mercury-constitutive equation. European Spallation Source (ESS), paper 81-T
10. Schoft S, Tepper J, Niayesh K (2005) Short circuit current limitation by means of liquid metal technology. In: Proceedings of 10th international conference on switching arc phenomenon, Lodz, pp 187–196
11. Awasthi A et al (1996) Measurement of contact angle in systems involving liquid metals. Meas Sci Technol 7:753–757
12. Ichinokawa T, Itoh H, Sakai Y (1999) Behaviors of small molten metal islands on several substrates. J Anal At Spectrom 14: 405–408
13. Karcher Ch, Kocourek V, Schulze D (2003) Experimental investigations of electromagnetic instabilities of free surfaces in a liquid metal drop. International Scientific Colloquium, Modelling for Electromagnetic Processing, Hannover
14. Kim J, Shen W, Latorre L, Kim Ch (2002) A micromechanical switch with electrostatically driven liquid-metal droplet. Sens Actuators A Phys 97–98: 672–679
15. leinhard JH (2006) A heat transfer textbook, 3rd edn. Phlogiston Press, Cambridge